JOC The Journal of Organic Chemistry

Article

pubs.acs.org/joc

Dual Photochemical Bond Cleavage for a Diarylethene-Based Phototrigger Containing both Methanolic and Acetic Sources

Olivier Galangau,[†] Stéphanie Delbaere,[‡] Nicolas Ratel-Ramond,[†] Gwénaël Rapenne,*[,†,§] Ruiji Li,[∥] Jan Patrick Dela Cruz Calupitan,[†,§,∥] Takuya Nakashima,[∥] and Tsuyoshi Kawai*[,†,∥]

[†]International Collaborative Laboratory for Supraphotoactive Systems, NAIST-CEMES, CNRS UPR 8011, 29 rue Marvig, F-31055 Toulouse Cedex 4, France

[‡]Université de Lille, CNRS UMR 8516 LASIR, 3, rue Pr. Laguesse, BP 83, 59006 Lille Cedex, France

[§]Université de Toulouse, UPS, 29 rue Marvig, F-31055 Toulouse Cedex 4, France

[∥]Graduate School of Materials Science, Nara Institute of Science and Technology, NAIST, 8916-5 Takayama-cho, Ikoma, Nara 630-0192, Japan

Supporting Information

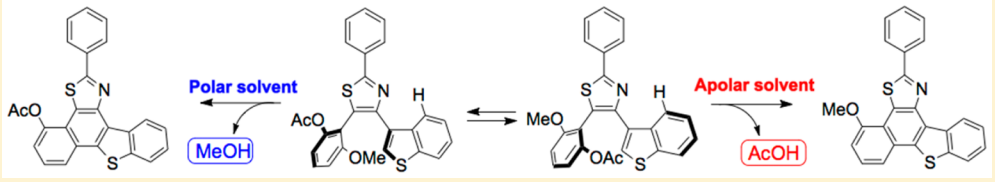

ABSTRACT: In this paper, we present a novel concept for "smarter" photolabile organic compounds combining not one but two caged functions. As proof of principle, this diarylethene-based compound possesses two inhibited chemical groups (OMe and OAc) and its efficient release in different solvents is reported. In low- to medium-polarity media, both MeOH and AcOH are released, with a slight preferential uncaging of AcOH except in 1,4-dioxane, where MeOH is preferentially released. In contrast, DMSO or DMF render AcOH release strongly dominating. DFT calculations of the corresponding photoreactive conformations not only afford strong support to the observed release of MeOH and AcOH but also qualitatively explain the preferential release of acid in terms of dispersive noncovalent interactions. Finally, mechanistic aspects are discussed on the bases of the spectroscopic observations and of the TD-DFT calculations.

INTRODUCTION

Phototriggers are common organic compounds extensively used to control dynamics of biological processes[1] and to trigger subsequent reactions such as polymerizations with photoacid generators[2] or photobase generators.[3] Photoactivatable molecules such as phototriggers usually incorporate an inhibited function, the so-called "caged" moiety, to be released after light absorption. The release process involves an irreversible bond breaking between the mother scaffold and the caged group. In turn, the uncaged function is therefore available for subsequent reaction. Tremendous efforts have already been devoted to optimize the relationship between the caged moiety and the molecular scaffold,[4] in order to obtain high quantum yields at absorption wavelengths located in the visible to NIR region[5] or to develop highly conjugated two-photon-absorbing phototriggers.[6] Wavelength-selective molecular systems were also successfully developed in the recent years.[7] In particular, Bochet et al.[8] clearly established drastic conditions to ensure a selective photocleavage: neither spectral overlap nor energy transfer should occur between the two caged groups. Therefore, this approach forbid any a priori combination of caged groups. In this paper, we proposed an alternative approach on the basis of our recent phototriggers (photoacid generator, PAG) based on a diarylethene pattern, in which the acidic source was bound to the reactive carbon sites (Figure 1).[9] After light absorption, our PAG prototypes underwent ring cyclization and immediate acidic elimination (MsOH, RCOOH, etc.) concomitant with the ring aromatization of the organic substrate, with an overall quantum yield of 0.5−0.7. Although this unique system was one of the most efficient to date in comparison to a compound reported by Marder et al.,[10] it was based on the very same classic phototrigger concept. In the present article, we report on the design and synthesis of a functionalized diarylethene which has been shown to be the first example of a dual photocleavable phototrigger. Our design, inspired by our previous development of highly photosensitive photochromic compounds, encompasses series of noncovalent interactions.[11] Therefore, as illustrated in Figure 2, N/H and O/S noncovalent interactions are introduced to stabilize the photoreactive conformers in solution.

To achieve the desired possibility of releasing two different molecules, two functionalities have been introduced on a phenyl ring which can rotate around a single C−C bond to switch from a stable conformer to another one. A conforma-

Received: September 13, 2016
Published: October 14, 2016

DOI: 10.1021/acs.joc.6b02256
J. Org. Chem. 2016, 81, 11282−11290

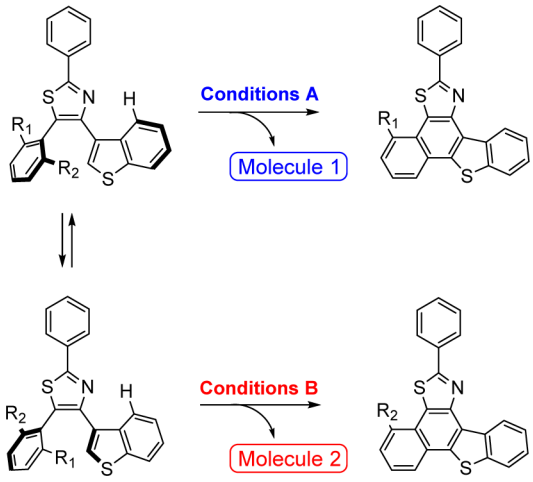

Figure 1. Principle of a dual photocleavable molecule based on a functional diarylethene derivative.

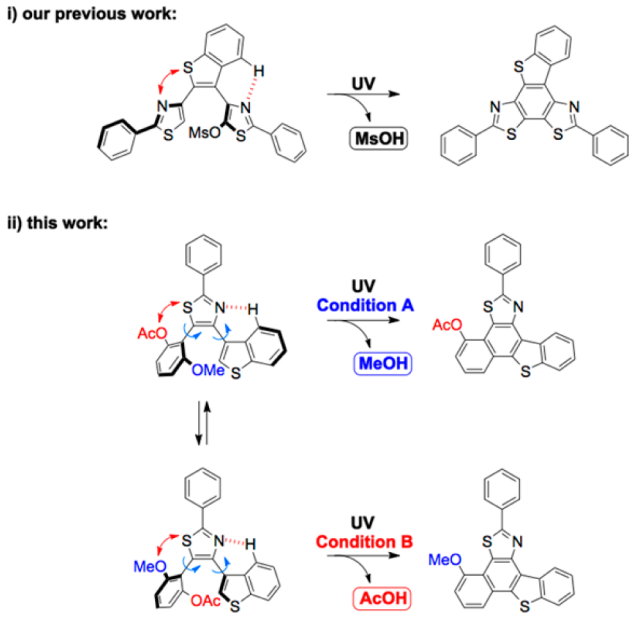

Figure 2. Illustration of the possibility of releasing two molecules from two different conformers of the same diarylethene starting material.

tional equilibrium between the two open isomers only in solution would allow for a proper selection of the function to be uncaged.

Note that the open isomers only enable the switch between the two photocleavable conformations, since they present the required flexibility, as opposed to their closed form counterpart. The presence of oxygen on both fragments will give an additional stability to both conformers through an efficient O/S interaction. Then, the presence of these two possible cyclization sites would give access selectively to the release of different molecules. As a proof of principle, two labile groups were incorporated in the final targets. In derivative **4**, which serves as a model compound, two identical groups (OMe) have been introduced at the reactive sites. In compound **6**, though, one OMe was replaced by OAc. To the best of our knowledge, this is the first successful design of second-generation phototriggers with dual photochemical pathways.

RESULTS AND DISCUSSION

Syntheses. Compound **6** with two different chemical groups (OAc and OMe) was obtained in five steps with a global yield of 67% (Scheme 1), whereas compound **4** with two OMe groups is the two-step precursor of **6**. To start with, 4-bromo-2-phenylthiazole (**1**) was coupled to commercially available 3-benzothienylboronic acid through Suzuki–Miyaura coupling. We have chosen 1,2-dimethoxyethane as solvent to activate the reaction, as was already reported in the literature.[12] Compound **2** was obtained in 98% yield and was selectively and cleanly brominated at the 5-position of the thiazolyl ring with *N*-bromosuccinimide to afford quasi-quantitatively compound **3**. The latter was further converted into our first target **4** thanks to the aforementioned Suzuki–Miyaura cross coupling, using commercially available 2,6-dimethoxybenzeneboronic acid. The first attempts to selectively deprotect one of the two OMe groups failed. BBr_3 in dichloromethane led to massive degradation, while using trimethylsilyl iodide in acetonitrile was uneffective on the substrate, either at room temperature or at reflux. Monodeprotection was finally achieved in excellent yield, using the conditions developed by Chae et al., giving compound **5** in 93% yield.[13] This single deprotection was confirmed by high-resolution mass spectroscopy (HRMS) and ^{1}H NMR (see the Supporting Information) with the presence of a singlet located at 3.56 ppm which has been assigned to the remaining OMe group and a broad signal at 5.14 ppm attributed to the phenolic proton. As expected, long reaction times did not afford the doubly deprotected compound as Chae et al. reported. Compound **5** was finally converted into **6** by acetylation conditions developed for bulky substrates, as standard acetylation did not afford the desired molecule. Therefore, acetyl chloride in the presence of tetrabutylammonium hydroxide and NaOH in CH_2Cl_2 gave **6** in a 91% yield.

X-ray Diffraction. Single crystals suitable for X-ray diffraction experiments (Figure 3) of derivatives **4** and **6** were grown from concentrated toluene solution by slowly diffusing vapors of MeOH, at room temperature.[14] Compound **4** crystallized in its antiparallel conformation, with evidence of series of stabilizing noncovalent interactions. Short distances were found consistent with N–H hydrogen bond and O–S interactions, as we expected. However, the rather high distance between the methoxy group and the benzothienyl plane ($d_{CH-\pi}$

Scheme 1. Reaction Pathway for Compounds 4 and 6

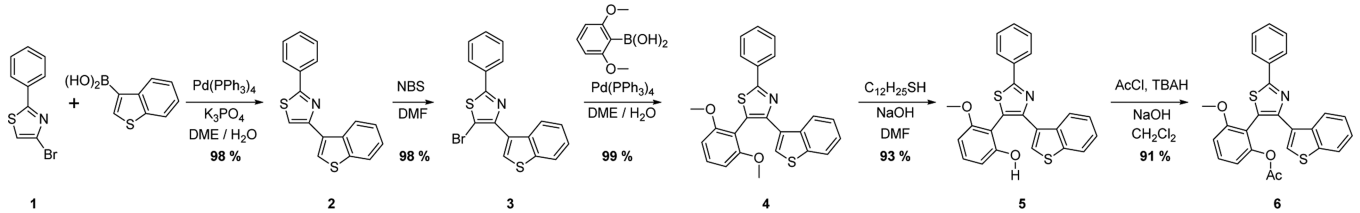

DOI: 10.1021/acs.joc.6b02256
J. Org. Chem. 2016, 81, 11282–11290

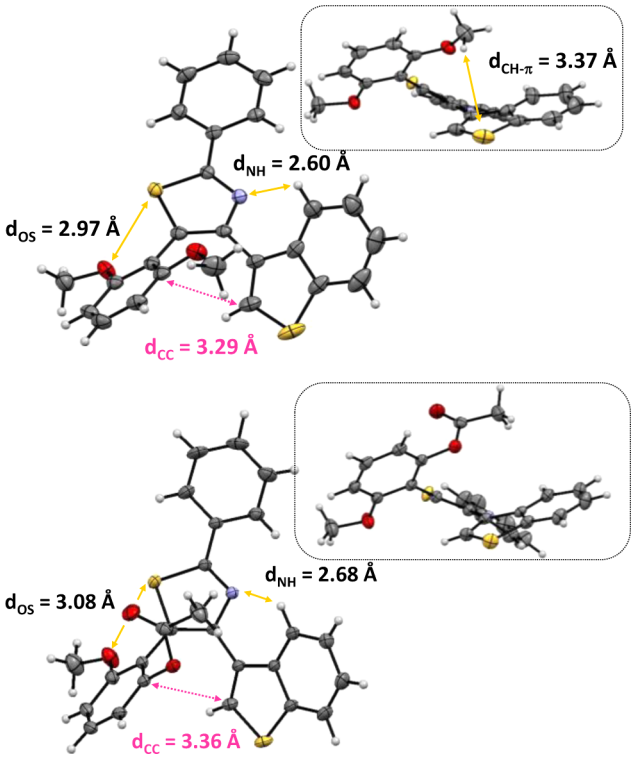

Figure 3. Thermal ellipsoid diagrams of compound **4** (top) and compound **6** (bottom). The ellipsoids are drawn at the 50% probability level. Double arrows represent the characteristic interactions along with the corresponding distances. Inset: CH−π distances.

= 3.4 Å) suggested a very weak CH−π interaction probably due to the repulsive "lone pair effect" of the oxygen.

Compound **6** also crystallized in a photoreactive conformation, that responsible for the release of AcOH. Thus, we could clearly conclude that this conformation at the origin of the release of AcOH was the most stable, at least in the crystal state. Note that no other conformers were found during the analysis, and irradiations of the crystals led to neither color modification nor morphological change. Similarly to **4**, several short distances were found consistent with intramolecular interactions, such as N−H hydrogen bonding and O−S interactions. No intramolecular CH−π interaction was observed. Instead, compound **6** packing displayed intermolecular S−H and N−H hydrogen bonding and CH−π interactions between adjacent molecules (not shown) involving the acetyl moiety and the thiazolyl ring, which probably prevented the formation of intramolecular CH−π interactions.

Spectroscopic Measurements. Compounds **4** and **6** were both studied in different solvents (toluene, 1,4-dioxane, THF, MeCN, and MeOH) at room temperature in aerated solutions. For both derivatives, open isomers **4o** and **6o** displayed absorption bands located in the UV part of the electromagnetic spectra, independent of the solvent used. All spectra showed a broad shoulder located in the red tail, followed by three absorption maxima located around 305, 295, and 260 nm (Figure 4).

In MeOH, the molar extinction coefficient of the first maximum is 13500 L mol^{-1} cm^{-1} for compound **4** and 16700 L mol^{-1} cm^{-1} for compound **6**. These values are characteristic and are associated with a spin-allowed π−π* transition, as supported by TD-DFT calculations. Absorption spectra and

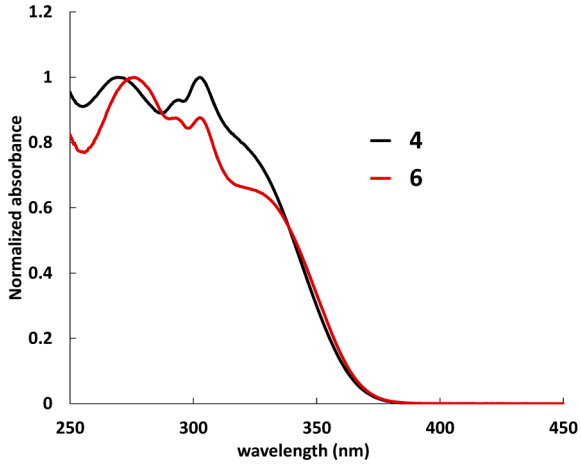

Figure 4. Normalized absorption spectra of compounds **4** and **6** in MeOH ($C = 10^{-5}$ mol/L, 298 K): (black line) compound **4**; (red line) compound **6**.

maxima are independent of the polarity of the solvent, as shown in Table 1 and the Supporting Information, which is in line with poor solvatochromic properties, as suggested by the TD-DFT calculations (vide infra). Indeed, vertical transitions leading to photocyclization are mainly of HOMO to LUMO character. These latter MOs have shown no charge transfer nature but correspond to electronic reorganization. Spectroscopic properties of compounds **4** and **6** are detailed in Table 1.

Photolysis Experiments on Compounds 4 and 6. Upon UV irradiation, spectra of both **4o** and **6o** in MeOH underwent a major change (Figure 5), with the emergence of several new bands in the UV part of the absorption spectra. Note that no band was seen in the visible part, meaning that, within the experimental time, the corresponding closed isomers **4c** and **6c**, with the cyclohexadiene structure, were not detected. Photoproduct **4a** was isolated and clearly identified by ^{1}H NMR in $CDCl_3$ as a fully aromatized organic system in which one molecule of MeOH was released from **4o**, as was already demonstrated by us several years ago on a similar derivative.[15] The loss of one MeOH molecule was also confirmed by HRMS. In the case of **6o**, two photoproducts were isolated and identified by ^{1}H NMR and HRMS as the previous photoproduct **4a**, on the one hand, and, on the other hand, the corresponding photoproduct **6a**, for which one MeOH molecule was released. Irradiation reactions are very clean, as judged by their NMR monitoring (vide infra). Assuming a quantitative reaction from **4o** to **4a**, we evaluated its absolute quantum yield of photolysis in MeOH to be ϕ_p = 0.25. This value fits well with the photoreactive conformer population at 298 K (22%) determined by VT-NMR in MeOH (see the Supporting Information). Altogether, **4o** and **6o** efficiently behave as phototriggers in MeOH. In particular, for compound **6o**, both MeOH and AcOH were released at room temperature.

We expanded our studies to other solvent polarities to gain further insight into the photochemical processes. For compound **4o**, irradiation in toluene, 1,4-dioxane, THF, and acetonitrile afforded an efficient release of MeOH in all of the solvents. However, as opposed to methanolic solutions (as in Figure 6 and the Supporting Information, for example), the reaction in THF showed a stepwise profile, with first the appearance of a band located in the visible region at around 560

DOI: 10.1021/acs.joc.6b02256
J. Org. Chem. 2016, 81, 11282−11290

Table 1. Extinction Coefficients and First Maxima of Absorption of Compounds 4o and 6o in Different Solvents

	extinction coeff (L mol^{-1} cm^{-1}) (λ (nm))				
	toluene	1,4-dioxane	THF	MeCN	MeOH
4o	15800 (305)	16300 (303)	21300 (304)	16700 (303)	13500 (303)
6o	17000 (303)	22600 (303)	18300 (303)	14800 (302)	16700 (303)

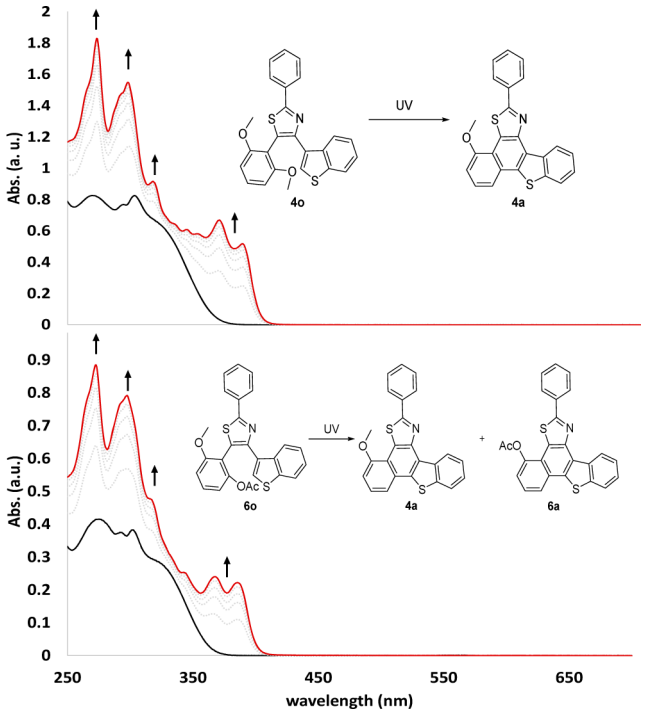

Figure 5. Photolysis experiments of compounds **4o** (top) and **6o** (bottom) in aerated MeOH (C = 10^{-5} mol/L, 298 K): (black line) open isomer; (red line) photostationary state.

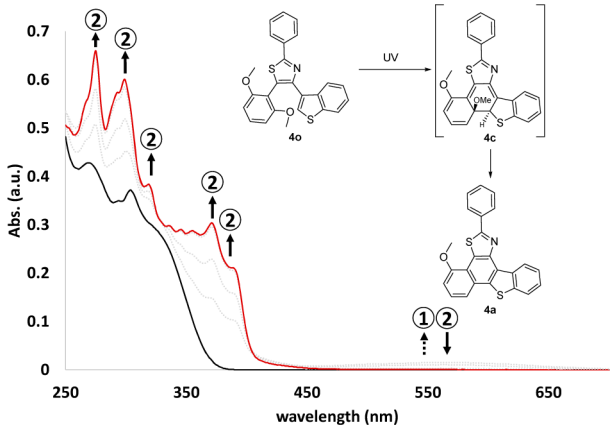

Figure 6. Photolysis experiments of compound **4o** in aerated THF (C = 10^{-5} mol/L, 298 K): (black line) open isomer; (red line) photostationary state. Circled numbers indicate the reaction stage.

nm, followed by the disappearance of this band and the growing of new bands in the UV region.

Irradiations of compound **6o** led to similar conclusions (Figure 7). Both AcOH and MeOH were efficiently released in all solvents used for this study. The photochemical bond cleavages seemed even more complex in toluene, 1,4-dioxane, and THF than in MeOH and MeCN (Figure 6 and the Supporting Information). As seen in THF solution (Figure 6),

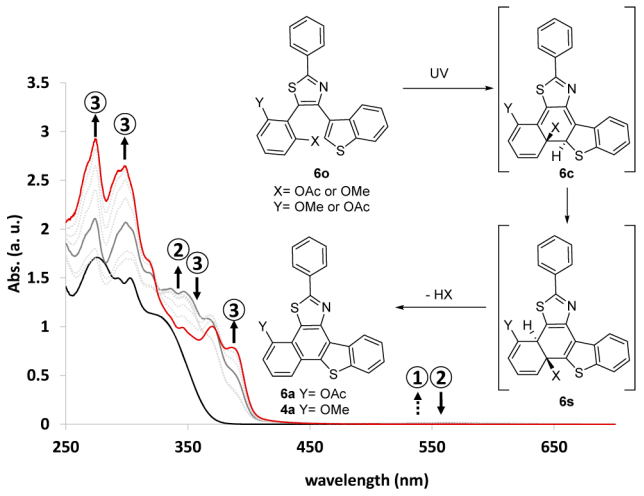

Figure 7. Photolysis experiments of compounds **6o** in aerated THF (C = 10^{-5} mol/L, 298 K): (black line) open isomer; (gray line) intermediate spectrum; (red line) photostationary state. Circled numbers indicate the reaction stage.

we roughly quantified three steps from the spectroscopic measurement of **6o**. First, the open isomer (**6o**) was converted into the closed isomer (**6c**), as immediately after UV irradiation a new band was observed in the visible range. Then, this band decreased with the appearance of three new bands located in the UV part with maxima at around 350 nm (**6s**). Finally, the latter vanished to give the final signature of the two photoproducts, namely **4a** and **6a** (see the Supporting Information for their absorption spectra). ^{1}H NMR and HRMS techniques allowed for a clear identification of those two final components (see the Supporting Information). With the support of DFT calculations (vide infra), we propose the following assignment for the three observed steps: (i) the formation of the closed isomer, as suggested by the appearance of an absorption band in the visible region, (ii) a [1,5]-proton shift, which should produce a nonphotochromic compound absorbing in the UV range (vide infra),[16] and (iii) the aromatization of the latter isomer concomitant with the release of MeOH and/or AcOH.

To conclude, both compounds behave as effective photo-triggers in the different solvents used. The release occurred at either low or high polarity. Except in a protic solvent such as MeOH, the photochemical processes involved the formation of the corresponding closed form, which is reactive enough at room temperature to immediately form the aromatic structure directly or form via the proton-shifting step. Although spectroscopic measurements afforded relevant qualitative results, we were interested in determining the solvent influence onto the elimination of AcOH and MeOH by means of NMR experiments.

NMR Data. Photoirradiations of **4o** and **6o** were monitored in a large variety (11) of deuterated solvents. UV irradiation induced large modifications in NMR spectra of the compounds **4** and **6**, due to the formation of the corresponding aromatized

DOI: 10.1021/acs.joc.6b02256
J. Org. Chem. 2016, 81, 11282−11290

forms and the concomitant release of MeOH and AcOH. Very clean reactions were observed, as judged by the NMR spectra. As illustrated in Figure 8, an intermediate species characterized

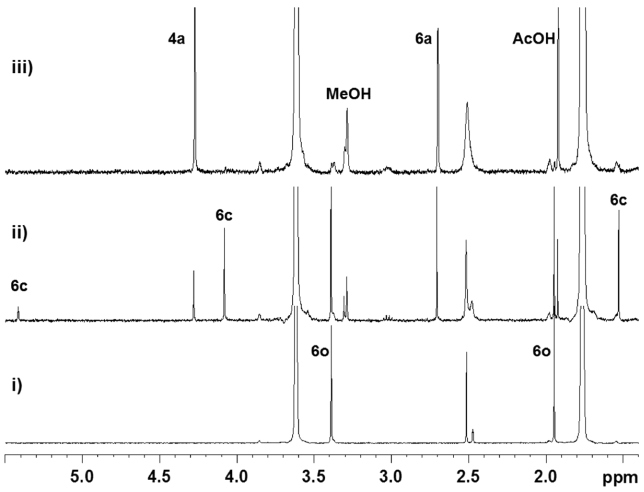

Figure 8. ^{1}H NMR spectra (aliphatic part) of compound **6o** in THF (C = 10^{-3} mol/L, 298 K): (i) before irradiation; (ii) after 10 min of irradiation; (iii) at the end of irradiation.

by signals at 5.41 ppm (1H), 4.1 ppm (O−CH_3), and 1.53 ppm (OAc) was detected. When it was stabilized at −60 °C in THF, 2D and NOE experiments allowed us to identify it as the corresponding closed isomer **6c_OAc** (see the Supporting Information). As a result, the appearance of the closed form isomer supports the spectrophotometric data. By an increase in the duration of irradiation, the initial compound **6o** can be fully converted into **4a** (δ(OMe) 4.28 ppm) and **6a** (δ(OAc) 2.7 ppm) concomitantly with MeOH (δ 3.29 ppm) and AcOH (δ 1.93 ppm). By measurement of the peak intensities of these four compounds, the ratio R = AcOH/MeOH could be calculated for the set of deuterated solvents used (Chart 1 and the Supporting Information).

Chart 1. Evaluation of the Ratio R = AcOH/MeOH (Striped Areas) as a Function of the Solvent Nature by ^{1}H NMR (C = 10^{-3} mol/L)

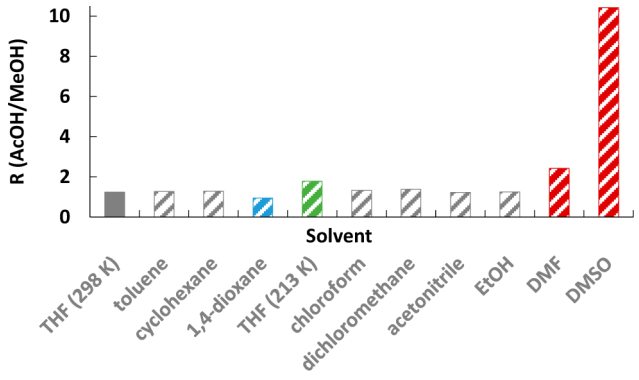

AcOH and MeOH were released in almost same ratio (R) independently of the solvent (Chart 1). Except in DMSO, DMF, and 1,4-dioxane, R was found to be around 1.3, resulting in a slight preferential release of AcOH at room temperature. In dioxane, R was evaluated to be 0.9, meaning that MeOH became slightly predominant as a photolabile group. Consequently, by choice of the appropriate solvent, the selectivity could be tuned. Moreover, the effect of temperature on the photoreaction selectivity was investigated. In THF, lowering the temperature from 25 to −60 °C induced a slight selectivity improvement in favor of AcOH. We interpreted this result as a more favorable stabilization of the AcOH-releasing photoreactive conformers by cooling the solution. This goes in line with the results extracted from XRD measurements and theoretical calculations. More importantly, DMF and DMSO induced a larger selectivity improvement with an R value of 2.4 (DMF) and more than 10 in DMSO. Such a result suggests that DMF and DMSO drove the conformational equilibrium at 298 K toward the AcOH uncaging conformer, probably thanks to series of dispersive interactions. In short, independently of the solvent, the photoreaction preferentially released AcOH. Choosing the appropriate conditions, though (solvent, temperature), allowed us to control the photoreaction selectivity.

Computational Details. DFT and TD-DFT calculations were performed with the Gaussian09 package.[17] We worked at the ωB97xD 6-31G(d,p) level of theory, since it is known to give accurate descriptions of DAE derivatives while taking into account dispersion forces.[18] Moreover, to model the bulk THF solvent effect on DFT, TD-DFT, and transient state calculations, we used the cost-effective PCM model. Optimizations of relevant structures were performed first, followed by IR calculations to ensure that the latter species corresponded to minima in energy. Vertical transitions were calculated from these minima. Conformational equilibria were also modeled at the ground state level by scanning the dihedral formed between the benzothienyl and thiazolyl central group. The QST2 formalism was used to calculate the transient state for the DAE [1,5]-proton shifts. Energetic comparisons are zero-point energy corrected. Ground state minima under vacuum for compounds **4o** and **6o** were found to correspond to open isomers in the photoreactive conformation, the so-called "antiparallel conformation" (Figures 9 and 10).

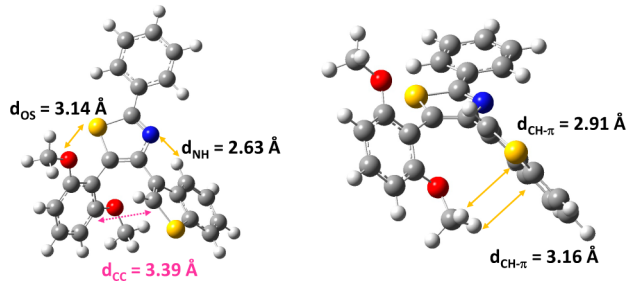

Figure 9. Antiparallel conformer of compound **4o**. Double arrows represent the characteristic distances and interactions.

In the case of **4o**, as anticipated, DFT calculations predicted series of noncovalent interactions such as N−H hydrogen bonds, O−S dispersive interactions (with the noteworthy interatomic distances lower than the sum of VDW radii) or CH−π interactions. Of particular interest is the distance separating the two reactive carbon sites (d_{CC}= 3.4 Å), which is close to that found in XRD experiments (d_{CC}= 3.3 Å). Theoretical calculations disclose another stable conformation, lying at +0.8 kcal mol^{-1} (see the Supporting Information). The corresponding structure resembles that called the "parallel" conformer, where the benzothienyl group is flipped with a secondary stabilizing N−H hydrogen bond. The small energy

DOI: 10.1021/acs.joc.6b02256
J. Org. Chem. 2016, 81, 11282−11290

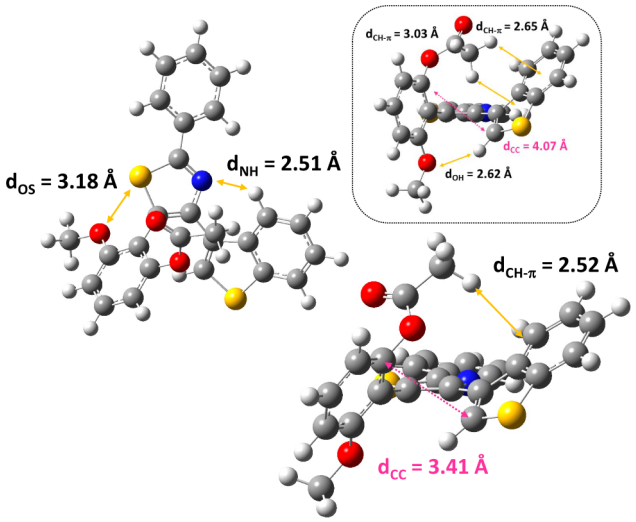

Figure 10. Antiparallel conformation **6o_OAc.** Double arrows represent the characteristic distances and interactions. Inset: secondary antiparallel conformation lying at +2 kcal/mol.

gap separating the two conformers suggested that a conformational equilibrium takes place in solution at room temperature, thus decreasing the quantum yield. Boltzmann analysis afforded a 79% population in favor of the antiparallel conformer (21% for the parallel conformer), which is the opposite ratio obtained by VT-NMR. However, solvent probably plays a crucial role in the conformational equilibrium and was not included in our calculations at the present level. In the case of **6o** under vacuum, the most stable conformer (**6o_OAc**) was found to be a photoreactive species (Figure 10) and was close to the XRD structure showed earlier. As for **4o**, an interplay of intramolecular interactions stabilized the conformation into its antiparallel configuration. Note also that a second antiparallel conformation was found lying at almost +2 kcal/mol, in which series of intramolecular interactions appeared.

Therefore, both conformations probably played an important role in the photoreactivity of compound **6o** in solution. A close examination of the ground state potential energy surface by scanning the dihedral angle formed between the benzothienyl and the central thiazole afforded three other potential conformations, all lying at higher energies (see the Supporting Information). This suggested that the total release efficiency might be diminished from **4o** to **6o**. Among them, two conformations are characterized by their parallel nature and the last conformation (**6o_OMe**) by its antiparallel nature (Figure 11).

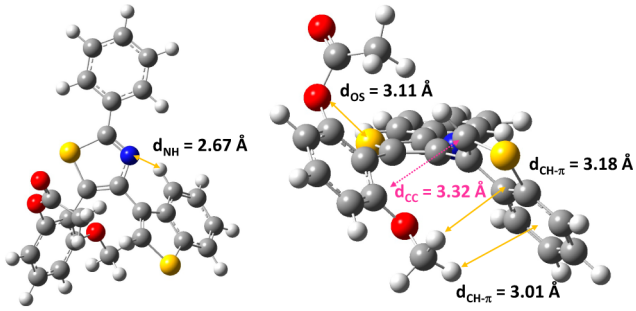

Figure 11. Antiparallel conformation **6o_OMe.** Double arrows represent the characteristic distances and interactions.

6o_OMe was characterized by a combination of noncovalent interactions, such as N−H, O−S, and CH−π. In this case, similarly to compound **4o**, d_{CC} decreased to 3.4 Å, making this conformation more ready to be involved in the desired photocyclization in comparison to **6o_OAc**. Overall, DFT calculations confirmed the existence of reactive conformations that may be responsible for the release of AcOH and MeOH. Therefore, the observations from NMR photolysis experiments can be qualitatively explained in terms of relative stabilities of these two respective conformers. In a low-polarity solvent, such as toluene, THF, or halogenated solvents, strong hydrogen bonds and O−S noncovalent tethering interactions should take place: hence, both conformers exist at room temperature and the corresponding release of AcOH and MeOH occurs in almost a 1:1 ratio. Furthermore, we suggest that CH−π interactions present in **6_OAc** give an extra stability to the system, resulting in the more efficient release of AcOH: hence the ratio of about 1.3. In addition, in DMSO or DMF, hydrogen bonding and O−S interactions should be weakened while CH−π interactions should be strengthened. In this regard, the energetic difference between **6o_OAc** and **6o_OMe** should be significantly elevated, resulting in a more predominant release of AcOH vs that of MeOH. Although this explanation fits well with the experimental data, it should also apply for solvents such as MeCN and EtOH. However, in the latter we found a ratio of 1.25. Therefore, further computational analyses including dynamic solvent effect must be undertaken to complete the picture.

TD-DFT calculations were also performed to examine the vertical transitions of **4o** and **6o**. We focused here only on the most stable conformers: namely, **4o** (antiparallel), **6o_OAc**, and **6o_OMe**. A solvent (THF) effect (bulk) was introduced. TD-DFT predicted vertical absorptions in rather good agreement with the experimental data (Table 2).

Table 2. Comparison of Theoretical and Experimental Absorption Maxima of Compounds 4, 6, 4a, and 6a in THF

	λ_{max}^{exp} (nm)	λ_{max}^{th} (nm)
4o	304	300
6o_OAc	303	298
6o_OMe	303	304
4c	570	480
6c_OAc	560	529
4a	390	321
6a	385	314

The largest discrepancy is obtained for isomer **4c** (Δ = ca. 0.4 eV), for which the transition is underestimated. This must be partially because of the rather broad absorption band shape and of difficulty in determining the absorption maxima precisely. As presented in the Supporting Information, the first transitions for **4o** and **6o_OAc** are dominated by the HOMO−LUMO character. These transitions can clearly be assigned to photochromic transitions, since one of the two reactive carbon sites in the LUMO presents enough density to perform the cyclization. Note as well that the transitions involved mainly electronic reorganization and hence no charge transfer character, which is in line with the observed spectroscopic properties.

The corresponding closed isomers (**4c** and **6c_OAc**) show a typical DAE closed form electronic signature, with the lowest energy transition associated with the cycloreversion process.

DOI: 10.1021/acs.joc.6b02256
J. Org. Chem. 2016, 81, 11282−11290

Indeed, the LUMOs are defined by an antibonding interaction between the two reactive carbon sites. More strikingly, HOMOs of **4c** and **6c_OAc** present very interesting topologies (Figure 12), where the remaining hydrogen atom engaged in

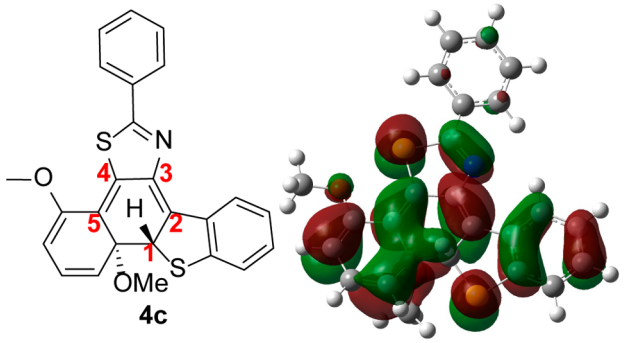

Figure 12. HOMO representation of isomer **4c**.

the photocyclization is somewhat incorporated into the π system's electron density. This HOMO distribution supports the possibility of the [1,5]-proton shift in the closed isomers **4c** and **6c_OAc**.

As a consequence, the corresponding [1,5]-proton-shifted isomers, namely **4s** and **6s**, were also implemented in our DFT description. Since both gave similar results, we will discuss only about the simplest case, **4s** (see the Supporting Information). **4s** is stabilized by 21 kcal mol^{-1} in comparison to **4o**. The shifted form is therefore more stable than the closed isomer **4c** generated after immediate photocyclization. Note that **4c** is lying at 32 kcal mol^{-1} higher in energy in comparison to **4o** (a complete energy diagram is given in the Supporting Information). A transient state for the thermal proton shift was also calculated (see the Supporting Information) and was found lying 28 kcal mol^{-1} higher than **4c**. Such an energetic barrier for the proton shift is similar to values reported in the literature and accordingly suggests that the proton shift might be a slow thermal rearrangement. This allows for proper detection at low temperature (vide supra).[19] TD-DFT of **4s** indicated a completely blue shifted vertical transition, with the lowest transition located at 300 nm representing a blue shift of almost 100 nm from **4c** to **4s**. Such a prediction fits well with observations in THF solution for the derivative **6**, for which the closed isomer disappeared to the benefit of a new species absorbing in the UV region (step 2). TD-DFT calculations were also performed for compounds **4a** and **6a**. Computed absorption maxima are in good agreement with the experimental values. Interestingly, computations reproduced the slight blue shift observed in solution on going from **4a** to **6a**. Frontier orbital topologies are characterized for both of them by large delocalization of the electron density over the entire structure, with no further photochromic activity.

Altogether, the computational data correlate very well with the observed electronic properties in solution for the different compounds and their various conformers. Calculations also foresee the existence of different photoreactive conformations responsible for the release of MeOH or AcOH. As a consequence, one could clearly imagine that changing the media's properties would affect the relative stabilities of these different conformations, therefore tuning in particular the ratio of AcOH/MeOH released after photocleavage. Finally, DFT also suggests a possible [1,5]-proton shift, which could be a key intermediate in the process of MeOH and/or AcOH release.

Conclusion. We have synthesized a unique phototrigger prototype, able to release both MeOH and AcOH in solution. We clearly succeeded in tuning the ratio of AcOH and MeOH released by photocleavage via a conformational control of the open isomer in DMSO or in DMF, though the solvent parameter responsible for such a phenomenon has to be unraveled. Tuning the AcOH/MeOH ratio was also achieved in a less pronounced way by changing the medium temperature. Thanks to spectrophotometric measurements, XRD techniques, NMR methods, and DFT calculations, we described qualitatively and quantitatively the elimination processes involved in the transformations. We strongly believe that our conceptual design of dual photocleavable molecules could pave the way for a new generation of organic multimode phototriggers.

EXPERIMENTAL SECTION

General Information. Commercially available chemicals were used without any further treatment. Dry solvents were purchased from commercial sources and kept under an argon atmosphere. HPLC grade solvents purchased commercially were used for purification and spectroscopic analyses. ^{1}H and ^{13}C NMR spectra and VT-NMR spectra were recorded on 300 and 400 MHz spectrometers. 1D (^{1}H and ^{1}D-ROESY) and 2D (^{1}H−^{1}H COSY, ^{1}H−^{13}C HSQC, ^{1}H−^{13}C HMBC, ^{1}H−^{1}H ROESY) NMR spectra (see the Supporting Information) were recorded on a 500 MHz spectrometer (^{1}H, 500 MHz; ^{13}C, 125 MHz) equipped with TXI, using standard sequences. Data sets were processed using commercial software. Chemical shifts were referenced to the residual solvent signals. Melting points were measured with a capillary system. Purifications by automatic flash chromatography were performed with HPLC-grade solvents. High-purity-grade silica (pore size of 60 Å, particle size of 40−63 μm) was used for manual flash chromatography. TLC analyses were achieved on silica gel (silica gel matrix containing a fluorescent indicator at 254 nm).

Photophysical Studies. Absorption spectra were recorded with a commercial spectrophotometer. A Hg−xenon lamp was used as an irradiation source (light power output of 3.8 W). Light of an appropriate wavelength was obtained by passing it through an additional filter (A9616-03 type, transmittance wavelength from 280 to 400 nm). Absolute ring cyclization quantum yield values were obtained on a commercial QYM setup.

Synthetic Procedures. *Synthesis of Compound* ***2***. A Schlenk tube equipped with a stirring bar was charged with the starting 4-bromo-2-phénylthiazole (1 g, 4.2 mmol, 1 equiv), the commercially available benzo[*b*]thiophen-3-ylboronic acid (1.1 g, 6.3 mmol, 1.5 equiv), and tripotassium phosphate (2.0 g, 9.4 mmol, 1.5 equiv) under argon. Dimethoxyethane (56 mL) was added, and the suspension was vigorously stirred and evacuated/back-filled with argon several times. $Pd(PPh_3)_4$ was added (0.22 g, 3 mol %), followed by the addition of distilled water (28 mL), and the solution was evacuated/back-filled with argon again and refluxed (oil bath temperature of 85 °C) over 24 h. As the reaction proceeded, the mixture turned purple. The mixture was cooled to room temperature and was partitioned between water and ethyl acetate. The organic phase was collected, dried over anhydrous $MgSO_4$, and filtered. The solvents were removed, and the crude mixture was purified by flash column chromatography (silica gel, CH_2Cl_2/hexane, 1/4 v/v) to afford a pale yellow viscous product (1.21 g, yield of 99%). R_f (CH_2Cl_2/hexane, 1/4 v/v) = 0.2. ^{1}H NMR (300 MHz, $CDCl_3$): δ 7.40−7.52 (m, 6H), 7.92−7.95 (m, 2H), 8.07−8.11 (m, 2H), 8.43−8.47 (m 1H). ^{13}C NMR (75 MHz, $CDCl_3$): δ 167.6, 151.6, 140.7, 137.1, 133.6, 131.2, 130.1, 128.9, 126.6, 125.4, 124.6, 124.5, 123.7, 122.8, 113.9. HRMS (CI-TOF): m/z 294.0411 calcd for $C_{17}H_{12}NS_2$ [M + H$^+$], found 294.0422.

Synthesis of Compound ***3***. Compound **2** (1.21 g, 4 mmol, 1 equiv) was dissolved in DMF (41 mL), and the resulting solution was cooled

DOI: 10.1021/acs.joc.6b02256
J. Org. Chem. 2016, 81, 11282−11290

to 0 °C. Neat *N*-bromosuccinimide (NBS) was added in one portion at the same temperature, and the mixture was slowly warmed to room temperature over 3 days. TLC monitoring of the reaction showed complete consumption of compound **2**. The crude mixture was partitioned between water and diethyl ether. The organic phase was washed with an aqueous solution of NaOH (approximately 1 M) and water. Then, the organic layers were dried over $MgSO_4$ and filtered and the solvents were removed. The solid crude mixture was purified by flash chromatography (silica gel, CH_2Cl_2/hexane, 1/4 v/v) to afford a viscous pale yellow solid (1.45 g, yield 95%). R_f (CH_2Cl_2/hexane, 1/4, v/v) = 0.5. Mp: 120 °C ± 1 °C. ^{1}H NMR (300 MHz, $CDCl_3$): δ 7.40−7.51 (m, 5H), 7.92−8.01 (m, 4H), 8.29−8.32 (m, 1H). ^{13}C NMR (75 MHz, $CDCl_3$): δ 167.2, 149.5, 139.8, 137.9, 133.0, 130.5, 129.0, 128.5, 127.5, 126.3, 126.2, 124.6, 124.5, 124.5, 124.5, 122.4, 105.4. HRMS (ESI-TOF): m/z 371.9516 calcd for $C_{17}H_{11}NBrS_2$ [M + H$^+$], found 371.9519.

Synthesis of Compound ***4***. A Schlenk tube equipped with a stirring bar was charged with compound **3** (1.5 g, 4.2 mmol, 1 equiv), the commercially available 2,6-dimethoxyphenylboronic acid (1.1 g, 6.1 mmol, 1.5 equiv), and tripotassium phosphate (1.9 g, 9.0 mmol, 1.5 equiv) under argon. Dimethoxyethane (54 mL) was added, and the suspension was vigorously stirred and evacuated/back-filled with argon several times. $Pd(PPh_3)_4$ was added (0.21 g, 3 mol %), followed by the addition of distilled water (27 mL), and the solution was evacuated/back-filled with argon again and refluxed (oil bath temperature of 85 °C) over 24 h. As the reaction proceeded, the mixture turned brown. When TLC monitoring showed reaction completion, the mixture was cooled to room temperature and was finally partitioned between water and EtOAc. The organic phase was collected, dried over $MgSO_4$, and filtered. The solvents were removed. The crude mixture was purified first by flash chromatography (silica gel, CH_2Cl_2/hexane, 1/3 v/v) and then by automatic flash chromatography (flow 5 mL/min, CH_2Cl_2/pentane, 1/9 v/v) to give a white solid (1.43 g, 82%). R_f (CH_2Cl_2/hexane, 1/1 v/v) = 0.3. Mp: 159 ± 1 °C. ^{1}H NMR (300 MHz, $CDCl_3$): δ 3.50 (s, 6H), 6.43 (d, J = 8.4 Hz, 2H), 7.15 (s, 1H), 7.23−7.45 (m, 7H), 7.79−7.82 (m, 1H), 8.05−8.08 (m, 2H), 8.26−8.29 (m, 1H). ^{13}C NMR (75 MHz, $CDCl_3$): δ 166.7, 158.5, 149.1, 139.7, 138.5, 134.1, 131.7, 130.3, 129.6, 128.8, 126.4, 125.8, 124.6, 124.4, 124.0, 122.1, 109.2, 104.0, 55.66. HRMS (ESI-TOF): m/z 430.0935 calcd for $C_{25}H_{20}NO_2S_2$ [M + H$^+$], found 430.0933.

Synthesis of Compound ***5***. A flame-dried Schlenk tube was charged with compound **4** (1.0 g, 2.3 mmol, 1 equiv), NaOH (0.56 g, 14 mmol, 6 equiv), and dry DMF (23 mL). The suspension was evacuated/back-filled with argon several times, and dodecanethiol (1.8 mL, 7.4 mmol, 3.2 equiv) was finally added dropwise via a syringe. The suspension was heated at 135 °C (oil bath temperature). After 1 h, TLC monitoring showed complete disappearance of the starting compound **4**. The suspension was cooled to room temperature and diluted with 1 N aqueous HCl solution. The aqueous layer was extracted several times with Et_2O, and the organic phases were recombined, dried over $MgSO_4$, and filtered. The solvents were removed, and the crude mixture was purified by flash column chromatography (silica gel, CH_2Cl_2/hexane, 1/1 v/v) to afford a white powder (0.96 g, yield 99%). R_f (CH_2Cl_2//hexane, 1/1 v/v) = 0.15. Mp: 153 ± 1 °C. ^{1}H NMR (300 MHz, $CDCl_3$): δ 3.56 (s, 3H, OMe), 5.14 (br s, 1H, OH), 6.40−6.44 (m, 2H), 7.10−7.41 (m, 7H), 7.72−7.75 (m, 1H), 7.97−8.00 (m, 2H), 8.32−8.36 (m, 1H). ^{13}C NMR (75 MHz, $CDCl_3$): δ 193.5, 168.5, 158.7, 154.7, 149.7, 139.9, 138.0, 133.6, 130.9, 130.2, 129.7, 128.9, 126.5, 125.8, 124.6, 124.4, 124.3, 123.5, 122.3, 108.6, 106.8, 103.1, 55.8. HRMS (ESI-TOF): m/z 416.0779 calcd for $C_{24}H_{18}NO_2S_2$ [M + H$^+$], found 416.0782.

Synthesis of Compound ***6***. A flame-dried Schlenk tube was charged with compound **5** (0.5 g, 1.2 mmol, 1 equiv), a catalytic amount of tetrabutylammonium hydrogen sulfate (TBAH), and NaOH (0.12 g, 3.0 mmol, 2.5 equiv). Dry 1,4-dioxane was added via a syringe, and the suspension was stirred at room temperature. Neat acetyl chloride (103 μL, 1.4 mmol, 1.2 equiv) was added dropwise via a syringe, and a white precipitate appeared. The mixture was stirred at room temperature until TLC monitoring showed reaction completion. The solids were filtered off and washed with CH_2Cl_2 or Et_2O, and the filtrate was concentrated under vacuum. The resulting crude mixture was purified first by flash column chromatography (silica gel, CH_2Cl_2/hexane, 1/1 to 2/1 v/v) and then by automatic flash column chromatography (silica gel, flow rate of 6−10 mL/min, CH_2Cl_2/pentane, 1/2 to 3/2). R_f (CH_2Cl_2/hexane, 1/1 v/v). Mp: 151 ± 1 °C. ^{1}H NMR (300 MHz, $CDCl_3$): δ 1.94 (s, 3H, OAc), 3.42 (s, 3H, OMe), 6.75−6.19 (m, 2H), 7.24 (s, 1H), 7.32−7.49 (m, 6H), 7.83−7.86 (m, 1H), 8.07−8.11 (m, 2H), 8.31−8.34 (m, 1H). ^{13}C NMR (75 MHz, $CDCl_3$): δ 168.8, 167.3, 158.4, 150.0, 149.7, 139.9, 138.2, 133.7, 130.7, 130.3, 130.0, 128.9, 128.8, 126.4, 125.6, 124.3, 124.2, 124.1, 123.8, 122.2, 115.1, 114.5, 108.8, 55.73, 20.60. HRMS (ESI-TOF): m/z 458.0885 calcd for $C_{26}H_{20}NO_3S_2$ [M + H$^+$], found 458.0883.

Synthesis of Compound ***4a***. A quartz round-bottom flask, equipped with a magnetic stirring bar and topped with a septum, was charged with 66 mg of compound **4** dissolved in approximately 25 mL of MeOH or THF. The solution, or in the case of MeOH the suspension, was bubbled with argon for 10 min with stirring. The solution (suspension) was then irradiated with UV light until TLC monitoring showed complete consumption of compound **4**. After 30 min of irradiation, TLC monitoring showed one new spot at R_f = 0.5 (CH_2Cl_2/hexane, 2/1, v/v). Mp: 240 ± 1 °C. The resulting crude product was purified by filtration on a silica pad ($CHCl_3$/hexane, 1/2 v/v), to afford a pale yellow powder. ^{1}H NMR (300 MHz, $CDCl_3$): δ 4.20 (s, 3H, OMe), 7.08 (dd, 1H, ^3J = 8.0 Hz, ^4J = 0.9 Hz), 7.43−7.72 (m, 6H), 7.84 (dd, 1H, ^3J = 8.0 Hz, ^4J = 0.9 Hz), 8.01 (ddd, 1H, ^3J = 8.0 Hz, ^4J_a = 1.3 Hz, ^4J_b = 0.7 Hz), 8.31−8.40 (m, 2H), 9.53 (ddd, 1H, 3J = 8.0 Hz, ^4J_a = 1.3 Hz, ^4J_b = 0.7 Hz). ^{13}C NMR (126 MHz, CD_3COCD_3): δ 170.0, 155.9, 149.2, 140.1, 137.5, 137.3, 135.1, 131.8, 131.1, 130.4, 129.0, 128.7, 128.1, 127.6, 127.4, 126.2, 123.6, 119.6, 118.1, 107.9, 56.8. HRMS (CI-TOF): m/z 398.0673 calcd for $C_{24}H_{16}NOS_2$ [M + H$^+$], found 398.0683.

Synthesis of Compound ***6a***. A quartz round-bottom flask, equipped with a magnetic stirring bar and topped with a septum, was charged with 53 mg of compound **6** dissolved in approximately 25 mL of MeOH or THF. The solution, or in the case of MeOH the suspension, was bubbled with argon for 10 min with stirring. The solution (suspension) was then irradiated with UV light until TLC monitoring showed complete consumption of compound **6**. TLC monitoring showed after 3 h of irradiation total disappearance of the starting material. The solvent was subsequently removed, and the crude product was purified by flash chromatography (silica gel, CH_2Cl_2/hexane, 2/1 v/v). Two compounds were generated, at R_f = 0.5 (CH_2Cl_2/hexane, 2/1 v/v) corresponding to compound **4a** and R_f = 0.1 (CH_2Cl_2/hexane, 2/1 v/v) corresponding to compound **6a**. Dec pt: >240 °C. ^{1}H NMR (300 MHz, $CDCl_3$): δ 2.65 (s, 3H), 7.37−7.74 (m, 8H), 7.98 (ddd, 1H, ^3J = 7.9 Hz, ^4J_a = 1.3 Hz, ^4J_b = 0.7 Hz, 1H), 8.08 (dd, 1H, ^3J = 7.9 Hz, ^4J = 1.1 Hz), 8.15−8.38 (m, 2H), 9.43 (ddd, 1H, ^3J = 8.0 Hz, ^4J_a = 1.4 Hz, ^4J_b = 0.7 Hz). ^{13}C NMR (126 MHz, CD_3COCD_3): δ 170.3, 169.7, 150.0, 147.1, 140.1, 138.0, 137.1, 134.6, 132.3, 130.4, 129.3, 128.7, 128.3, 128.0, 127.9, 127.4, 126.3, 124.5, 123.7, 123.6, 121.8, 22.2. HRMS (CI-TOF): m/z 426.0609 calcd for $C_{25}H_{16}NO_2S_2$ [M + H$^+$], found 426.0622.

■ ASSOCIATED CONTENT

Supporting Information

The Supporting Information is available free of charge on the ACS Publications website at DOI: 10.1021/acs.joc.6b02256.

X-ray crystallographic file for compound **4** (CIF)
X-ray crystallographic file for compound **6** (CIF)
Photoirradiation experiments, NMR spectra, VT-NMR study, UV−visible experiments, and computational details (PDF)

■ AUTHOR INFORMATION

Corresponding Authors

*E-mail for G.R.: rapenne@cemes.fr.
*E-mail for T.K.: tkawai@ms.naist.jp.

DOI: 10.1021/acs.joc.6b02256
J. Org. Chem. 2016, 81, 11282−11290

Notes

The authors declare no competing financial interest.

■ ACKNOWLEDGMENTS

Financial support for this work was supported by the NAIST Foundation, the CNRS, the University Paul Sabatier (Toulouse), and the Programme Investissements d'Avenir ANR-11-IDEX-0002-02, reference ANR-10-LABX-0037-NEX. The authors are also grateful to Dr. Vedrennes for his help with VT-NMR measurements. T.K. acknowledges financial support by the JSPS KAKENHI (Grant Number JP26107006) in Scientific Research on Innovative Areas "Photosynergetics".

■ REFERENCES

(1) (a) Bochet, G. C. *Pure Appl. Chem.* **2006**, *78*, 241−247. (b) Yu, H.; Li, J.; Wu, D.; Qiu, Z.; Zhang, Y. *Chem. Soc. Rev.* **2010**, *39*, 464−473 and references cited therein. (c) Pelliccioli, P.; Wirz, J. *Photochem. Photobiol. Sci.* **2002**, *1*, 441−458 and references therein. (d) Ellis-Davies, G. C. R. *Nat. Methods* **2007**, *4*, 619−628. (e) Mayer, G.; Heckel, A. *Angew. Chem., Int. Ed.* **2006**, *45*, 4900−4921. (f) Bao, C.; Zhu, L.; Lin, Q.; Tian, H. *Adv. Mater.* **2015**, *27*, 1647−1662 and references therein.

(2) (a) Roffey, C. G. *Photogeneration of Reactive species for UV curing*; Wiley: New York, 1997. (b) Fouassier, J.-P. *Photoinitiation, Photopolymerization and Photocuring: Fundamentals and Applications*; Hanser: Munich, Germany, 1995. (c) Crivello, J. V. *Photoinitiators for Free Radical, Cationic and Anionic Photopolymerization*; Wiley: New York, 1998. (d) Ito, H.; Willson, C. G.; Frechet, J. M. J.; Farrall, M. J.; Eichler, E. *Macromolecules* **1983**, *16*, 510−517. (e) For reviews, see: Crivello, V. J.; Reichmanis, E. *Chem. Mater.* **2014**, *26*, 533−548. Wallraff, G. M.; Hinsberg, W. D. *Chem. Rev.* **1999**, *99*, 1801−1822.

(3) For recent reviews, see: (a) Suyama, K.; Shirai, M. *Prog. Polym. Sci.* **2009**, *34*, 194−209. (b) Kutal, C. *Coord. Chem. Rev.* **2001**, *211*, 353−368. For recent examples, see: (c) Sun, W.; Gao, J. P.; Wang, Z. Y. *J. Am. Chem. Soc.* **2008**, *130*, 8130−8131. (d) Arimitsu, K.; Endo, R. *Chem. Mater.* **2013**, *25*, 4461−4463. (e) Hagiwara, Y.; Mesch, A. R.; Kawakami, T.; Okazaki, M.; Jockush, S.; Li, Y.; Turro, J. N.; Willson, C. G. *J. Org. Chem.* **2013**, *78*, 1730−1734. (f) Turro, J. N.; Li, Y.; Jockush, S.; Hagiwara, Y.; Okazaki, M.; Schuster, I. D.; Willson, C. G. *J. Org. Chem.* **2013**, *78*, 1735−1741.

(4) (a) Zhang, Y.; Captain, B.; Raymo, M. F. *Adv. Opt. Mater.* **2016**, *4*, 1363. (b) Impellizzeri, S.; McCaughan, B.; Callan, F. J.; Raymo, M. F. *J. Am. Chem. Soc.* **2012**, *134*, 2276−2283.

(5) (a) Klán, P.; Šolomek, T.; Bochet, C. G.; Blanc, A.; Givens, T.; Rubina, M.; Popik, V.; Kostikov, A.; Wirz, J. *Chem. Rev.* **2013**, *113*, 119−191. (b) Shembekar, V. R.; Chen, Y.; Carpenter, B. K.; Hess, G. P. *Biochemistry* **2005**, *44*, 7107−7114. (c) Hagen, V.; Dekowski, B.; Nache, V.; Schmidt, R.; Geißler, D.; Lorenz, D.; Eichhorst, J.; Keller, S.; Kaneko, H.; Benndorf, K.; Wiesner, B. *Angew. Chem., Int. Ed.* **2005**, *44*, 7887−7891. (d) Hagen, V.; Dekowski, B.; Kotzur, N.; Lechler, R.; Wiesner, B.; Briand, B.; Beyermann, M. *Chem. - Eur. J.* **2008**, *14*, 1621−1627.

(6) (a) Härtner, S.; Kim, H.-C.; Hampp, N. *J. Polym. Sci., Part A: Polym. Chem.* **2007**, *45*, 2443−2452. (b) Fournier, L.; Gauron, C.; Xu, L.; Aujard, I.; Le Saux, T.; Gagey-Eilstein, N.; Maurin, S.; Dubruille, S.; Baudin, J.-B.; Bensimon, D.; Volovitch, M.; Vriz, S.; Jullien, L. *ACS Chem. Biol.* **2013**, *8*, 1528−1536. (c) Olson, J. P.; Kwon, H.-B.; Takasaki, K. T.; Chiu, C. Q.; Higley, M. J.; Sabatini, B. L.; Ellis-Davies, G. C. R. *J. Am. Chem. Soc.* **2013**, *135*, 5954−5957. (d) Furuta, T.; Wang, S. S.-H.; Dantzker, J. L.; Dore, T. M.; Bybee, W. J.; Callaway, E. M.; Denk, W.; Tisen, R. Y. *Proc. Natl. Acad. Sci. U. S. A.* **1999**, *96*, 1193−1200.

(7) (a) Bochet, C. G. *Tetrahedron Lett.* **2000**, *41*, 6341−6346. (b) Blanc, A.; Bochet, C. G. *J. Org. Chem.* **2002**, *67*, 5567−5577. (c) Blanc, A.; Bochet, C. G. *Org. Lett.* **2007**, *9*, 2649−2651. (d) Kotzur, N.; Briand, B.; Beyermann, M.; Hagen, V. *J. Am. Chem. Soc.* **2009**, *131*, 16927−16931. (e) Stanton-Humphreys, M. N.; Taylor, R. D. T.; McDougall, C.; Hart, M. L.; Brown, C. T. A.; Emptage, N. J.; Conway, S. J. *Chem. Commun.* **2012**, *48*, 657−659. (f) Olson, J. P.; Banghart, M. R.; Sabatini, B. L.; Ellis-Davies, G. C. R. *J. Am. Chem. Soc.* **2013**, *135*, 15948−15954.

(8) Bochet, C. G. *Angew. Chem., Int. Ed.* **2001**, *40*, 2071−2073.

(9) (a) Nakashima, T.; Tsuchie, K.; Kanazawa, R.; Li, R.; Iijima, S.; Galangau, O.; Nakagawa, H.; Mutoh, K.; Kobayashi, Y.; Abe, J.; Kawai, T. *J. Am. Chem. Soc.* **2015**, *137*, 7023−7026. (b) Li, R.; Nakashima, T.; Kanazawa, R.; Galangau, O.; Kawai, T. *Chem. - Eur. J.* **2016**, DOI: 10.1002/chem.201603768.

(10) Zhou, W.; Kuebler, S. M.; Carrig, D.; Perry, J. W.; Marder, S. R. *J. Am. Chem. Soc.* **2002**, *124*, 1897−1901.

(11) (a) Fukumoto, S.; Nakashima, T.; Kawai, T. *Angew. Chem., Int. Ed.* **2011**, *50*, 1565−1568. (b) Galangau, O.; Kanazawa, R.; Kimura, Y.; Nakashima, T.; Kawai, T. *Eur. J. Org. Chem.* **2014**, *2014*, 7165−7173. (c) Li, R.; Nakashima, T.; Galangau, O.; Iijima, S.; Kanazawa, R.; Kawai, T. *Chem. - Asian J.* **2015**, *10*, 1725−1730.

(12) (a) Galangau, O.; Nakashima, T.; Maurel, F.; Kawai, T. *Chem. - Eur. J.* **2015**, *21*, 8471−8482. (b) Sanz, R.; Guilarte, V.; Hernando, E.; Sanjuán, A. M. *J. Org. Chem.* **2010**, *75*, 7443−7446. (c) Heynderickx, A.; Samat, A.; Guglielmetti, R. *Synthesis* **2002**, *2002*, 213−216.

(13) Chae, J. *Arch. Pharmacal Res.* **2008**, *31*, 305−309.

(14) (a) Crystallographic data for compound **4**: $C_{26}H_{19}NO_3S_2$, a = 10.7644(5) Å, b = 16.2126(7) Å, c = 24.4126(13) Å, V = 4260.5(4) Å^3, α = 90°, β = 90°, γ = 90°, ρ_{calcd} = 1.339 g/cm^3, space group $Pb2_1a$. Hydrogen atoms were calculated in riding positions. CCDC-1483014 contains supplementary crystallographic data for this paper. These data can be obtained free of charge from www.ccdc.cam.ac.uk/data_request/cif. (b) Crystallographic data for compound **6**: $C_{26}H_{19}NO_3S_2$, a = 13.9787(5) Å, b = 8.8699(3) Å, c = 17.8770(6) Å, V = 2211.22(13) Å^3, α = 90°, β = 93.978(1)°, γ = 90°, ρ_{calcd} = 1.374 g/cm^3, space group $P2_1/a$. Hydrogen atoms were calculated in riding positions. CCDC-1485482 contains supplementary crystallographic data for this paper. These data can be obtained free of charge from www.ccdc.cam.ac.uk/data_request/cif.

(15) (a) Nakagawa, H.; Kawai, S.; Nakashima, T.; Kawai, T. *Org. Lett.* **2009**, *11*, 1475−1478. (b) Nakagawa, H.; Nakashima, T.; Kawai, T. *Eur. J. Org. Chem.* **2012**, *2012*, 4493−4500.

(16) Lvov, A. G.; Shirinian, V. Z.; Kachala, V. V.; Kavun, A. M.; Zavarzin, I. V.; Krayushkin, M. M. *Org. Lett.* **2014**, *16*, 4532−4535.

(17) See the Supporting Information for the full reference.

(18) (a) Chantzis, A.; Cerezo, J.; Perrier, A.; Santoro, F.; Jacquemin, D. *J. Chem. Theory Comput.* **2014**, *10*, 3944−3957. (b) Li, X.; Zou, Q.; Ågren, H. *J. Phys. Chem. A* **2015**, *119*, 9140−9147.

(19) Alabugin, I. V.; Manoharan, M.; Breiner, B.; Lewis, F. D. *J. Am. Chem. Soc.* **2003**, *125*, 9329−9342.

DOI: 10.1021/acs.joc.6b02256
J. Org. Chem. 2016, 81, 11282−11290